



**Queensland University of Technology**  
Brisbane Australia

This is the author's version of a work that was submitted/accepted for publication in the following source:

Frost, Ray L., Martens, Wayde N., Ding, Zhe, & Kloprogge, J. Theo (2003) DSC and high-resolution TG of synthesized hydrotalcites of Mg and Zn. *Journal of Thermal Analysis and Calorimetry*, 71(2), pp. 429-438.

This file was downloaded from: <http://eprints.qut.edu.au/22050/>

© Copyright 2003 Akademiai Kiado Rt. (Springer)

**Notice:** *Changes introduced as a result of publishing processes such as copy-editing and formatting may not be reflected in this document. For a definitive version of this work, please refer to the published source:*

<http://dx.doi.org/10.1023/A:1022835305846>

# Differential scanning calorimetry and high-resolution thermogravimetric analysis of synthesized hydrotalcites of Mg and Zn

R. L. Frost\*, W. Martens, Z. Ding, J. T. Kloprogge

*Centre for Instrumental and Developmental Chemistry, Queensland University of Technology, 2 George Street, Brisbane, GPO Box 2434, Queensland 4001, Australia.*

## Abstract

A combination of DSC and high resolution DTGA coupled to a gas evolution mass spectrometer has been used to study the thermal properties of a series of Mg/Zn hydrotalcites of formulae  $Mg_xZn_{6-x}Al_2(OH)_{16}(CO_3).4H_2O$  where x varied from 6 to 0. The effect of increased Zn composition results in the decrease of the endotherms and weight loss steps to lower temperatures. Evolved gas mass spectrometry shows that water is lost in a number of steps. The interlayer carbonate anion is lost simultaneously with hydroxyl units.

**Keywords:** dehydration, dehydroxylation, hydrotalcite, differential scanning calorimetry, high-resolution thermogravimetric analysis

## Introduction

Hydrotalcites, or layered double hydroxides (LDH) are fundamentally anionic clays, and are less well-known and more diffuse in nature than cationic clays like smectites. The structure of hydrotalcite can be derived from a brucite structure ( $Mg(OH)_2$ ) in which e.g.  $Al^{3+}$  or  $Fe^{3+}$  (pyroaurite-sjögrenite) substitutes a part of the  $Mg^{2+}$ . This substitution creates a positive layer charge on the hydroxide layers, which is compensated by interlayer anions or anionic complexes. In hydrotalcites a broad range of compositions are possible of the type  $[M^{2+}_{1-x}M^{3+}_x(OH)_2][A^{n-}]_{x/n}.yH_2O$ , where  $M^{2+}$  and  $M^{3+}$  are the di- and trivalent cations in the octahedral positions within the hydroxide layers with x normally between 0.17 and 0.33.  $A^{n-}$  is an exchangeable interlayer anion [1, 2].

Hydrotalcites both natural and synthetic have been known for an extended period of time [3, 4]. Likewise the characterisation of these types of minerals by thermal analysis goes back in time [5-7]. In this work [7] a naturally occurring hydrotalcite from Snarum in Norway of formula  $2CO_2.Al_2O_3.8MgO.20H_2O$ , near that of stichtite. Thermal analysis showed two endothermic peaks, at 180°C and at 480°C; the first endotherm corresponds to dehydration, the second to loss of  $CO_2$ . The dehydration produces destruction of the lattice and the product is not crystalline as determined by X-ray diffraction. In more recent times the mass spectrometric analysis of evolved gases enabled the decomposition of the hydrotalcites to be correlated with thermal analysis [8]. These analyses showed the temperature range over which various gases were evolved.

---

\* Author to whom correspondence should be addressed (r.frost@qut.edu.au)

Importantly, the use of hydrotalcites in the synthesis of nanocomposites has enabled high temperature phase composite materials to be manufactured [9, 10]. The addition of hydrotalcites to polymeric materials can result in thermally stable nanocomposite materials. Important to this work is the knowledge of when the hydrotalcite decomposes and the mechanisms for this decomposition. This decomposition temperature influences the temperature of the formation of this nanocomposite. This research complements our studies in the synthesis and characterisation of hydrotalcites [11]. In this work we report the high-resolution thermogravimetric analysis of a series of hydrotalcites with different Mg and Zn ratios.

## **EXPERIMENTAL**

### **Synthesis of hydrotalcite samples**

Hydrotalcites with a composition of  $Mg_xZn_{6-x}Al_2(OH)_{16}(CO_3) \cdot 4H_2O$  where  $x$  varied from 6 to 0, were synthesised by the coprecipitation method. Three solutions were prepared, solution 1 contained 2M NaOH and 0.125M  $Na_2CO_3$ , solution 2 contained 0.75M  $Mg^{2+}$  ( $Mg(NO_3)_2 \cdot 6H_2O$ ) together with 0.25M  $Al^{3+}$  ( $Al(NO_3)_3 \cdot 9H_2O$ ), solution 3 contained 0.75M  $Zn^{2+}$  with 0.25M  $Al^{3+}$  ( $Al(NO_3)_3 \cdot 9H_2O$ ). Solution 2 and 3 in the appropriate ratio were added to solution 1 using a peristaltic pump at a rate of  $40 \text{ cm}^3/\text{min}$ ., under vigorous stirring, maintaining a pH of 10. Hydrothermal treatment of the hydrotalcites was achieved by using Parr reactors at an autogenous water vapour pressure at  $150^\circ\text{C}$ , in Teflon lined stainless steel reactors for 14 days. The samples were analysed for chemical composition with an electron microprobe and for phase composition by X-ray diffraction.

### **Thermal Analysis**

Thermal decomposition of the hydrotalcite was carried out in a TA high-resolution thermogravimetric analyzer (series Q500) in a flowing nitrogen atmosphere ( $80 \text{ cm}^3/\text{min}$ ) at a pre-set, constant decomposition rate of  $0.15 \text{ mg}/\text{min}$ . (Below this threshold value the samples were heated under dynamic conditions at a uniform rate of  $0.5 \text{ }^\circ\text{C}/\text{min}$ ). The samples were heated in an open platinum crucible at a rate of  $0.5 \text{ }^\circ\text{C}/\text{min}^{-1}$  up to  $500^\circ\text{C}$ . With the quasi-isothermal heating program of the instrument the furnace temperature was regulated precisely to provide a uniform rate of decomposition in the main decomposition stage. The TGA instrument was coupled to a Balzers (Pfeiffer) mass spectrometer for gas analysis. Only selected gases, namely water and carbon dioxide, were analyzed.

Differential Scanning Calorimetry (DSC) was performed on a TA® Instrument DSC Q10 analyser. Sample powders were loaded into sealed alumina pan and heated to  $500^\circ\text{C}$  at heating rate of  $2^\circ\text{C}/\text{min}$ . The empty alumina pan was used as reference and the heat flow between the sample and reference pans was recorded.

## **Results and discussion**

### ***Differential Scanning Calorimetry***

Minerals such as the synthesised hydrotalcites decompose at low temperatures and lend themselves to differential scanning calorimetry. Figure 1 displays the analyses of the Mg/Zn hydrotalcites and the results of the peak fitting of the analyses are reported in Table 1. Both the figure and the table clearly show that the thermal decomposition is complex with many overlapping peaks. It is convenient to subdivide the data in accordance with the temperature range: (a) steps below 110°C (b) steps from 110 to 200°C (c) steps between 200 and 300°C and steps above 300°C. For the Mg hydrotalcite ( $\text{Mg}_6\text{Al}_2(\text{OH})_{16}(\text{CO}_3)\cdot 4\text{H}_2\text{O}$ ) two predominant heat flow steps are observed at 57 and around 90°C. These two heat flow steps are attributed to adsorbed water and to interlayer water. Upon substitution of the Mg by Zn according to the formulae:  $\text{Mg}_4\text{Zn}_2\text{Al}_2(\text{OH})_{16}(\text{CO}_3)\cdot 4\text{H}_2\text{O}$ , the heat flow steps are observed at 75 and 93°C. Upon increased Zn substitution according to the formulae:  $\text{Mg}_2\text{Zn}_4\text{Al}_2(\text{OH})_{16}(\text{CO}_3)\cdot 4\text{H}_2\text{O}$ , heat flow loss steps are observed at 69, 91 and 98°C. An additional step is also observed at 105°C. When the Mg has been completely replaced with Zn, the low temperature heat flow steps are observed at 58, 67 and 108°C.

The question arises as to why there are many heat flow steps. Later in this manuscript it is shown that these heat flow steps are attributed to water loss. The hydrotalcite structure is based upon the brucite structure such that some of the Mg is replaced by Al. In other words  $\text{Mg}(\text{OH})_2\cdot x\text{H}_2\text{O}$  becomes  $\text{Mg}_6\text{Al}_2(\text{OH})_{16}(\text{CO}_3)\cdot 4\text{H}_2\text{O}$ . A number of questions arise as to the siting of the Mg and Al in the hydrotalcite structure. Are the aluminium cations well separated by the Mg or do the cations form aggregations of Mg and Al in the layers? The observation of several heat loss steps in the temperature range up to 110°C suggests that the water is adsorbed differently on the MgOH and AlOH units. Some of this water may be structural water hydrogen bonded to the MOH units. The observation of several heat flow steps for the hydrotalcites suggests the interlayer adsorbed water is being lost at a number of temperatures.

Hydrotalcite ( $\text{Mg}_6\text{Al}_2(\text{OH})_{16}(\text{CO}_3)\cdot 4\text{H}_2\text{O}$ ) shows a heat flow step at 131°C, which is also attributed to water loss. This water molecule is chemically bonded to the hydrotalcite surface. On the Mg/Zn 4:2 hydrotalcite this heat flow step is observed at 144°C. Other steps are observed at 172 and 184°C. On the Mg/Zn 2:4 hydrotalcite heat flow steps are observed at 174, 186 and 196°C. For the ( $\text{Zn}_6\text{Al}_2(\text{OH})_{16}(\text{CO}_3)\cdot 4\text{H}_2\text{O}$ ) hydrotalcite, multiple heat flow steps are observed at 161, 178 and 218°C. Two higher temperature heat flow steps are observed at around 256°C and 340°C. These steps are assigned to the loss of hydroxyls from the structure and from the loss of carbon dioxide from the interlayer anion. Three overlapping heat flow steps are observed for ( $\text{Mg}_6\text{Al}_2(\text{OH})_{16}(\text{CO}_3)\cdot 4\text{H}_2\text{O}$ ) at 256, 260 and 269°C. For the Zn substituted hydrotalcites, this heat flow step is observed at 260, 250 and 218°C. It is concluded that as the Mg is substituted by Zn, there is a tendency for the heat flow steps to occur at lower temperatures.

### ***High Resolution Thermogravimetric Analysis***

The high-resolution thermogravimetric analyses of the hydrotalcites are shown in Figure 2. The results of the analysis of these DTGA curves are reported in Table 2. In many respects the DTGA patterns follow the DSC patterns. The data may be analysed in a similar fashion to that of the DSC. The weight loss steps may also be

divided into below 110°C and above 110°C. Three weight loss steps are observed for the Mg hydrotalcite at 40, 84 and 112°C. Above 110°C, two weight loss steps are observed at 246 and 261°C with higher temperature weight loss steps at 307 and 336. The theoretical weight losses for a hydrotalcite of formula  $(\text{Mg}_6\text{Al}_2(\text{OH})_{16}(\text{CO}_3)\cdot 4\text{H}_2\text{O})$  are 12.0% for  $\text{H}_2\text{O}$ , 10% for  $\text{CO}_2$  and 45% for the OH units. The weight loss step at 112°C shows a weight loss step of 12.3%, which fits well with the theoretical value. The weight loss at lower temperatures corresponds to adsorbed water. The weight loss step at 336°C is 18.3%, which is too high for the loss of  $\text{CO}_2$  alone. The application of infrared spectroscopy to the study of hydrotalcites has shown that the carbonate is strongly bonded to the interlayer water and to the hydroxyl units in the structure. A predicted weight loss of 10% is not found as mass spectrometry shows the hydroxyl units and  $\text{CO}_2$  are released simultaneously. Addition of the weight losses at 246, 261, and 307°C comes to 37.3%, which approaches the expected value of 45%.

For the  $\text{Mg}_4\text{Zn}_2\text{Al}_2(\text{OH})_{16}(\text{CO}_3)\cdot 4\text{H}_2\text{O}$  hydrotalcite, weight loss steps of 4.5, 7.2, 7.6, and 9.1% are observed at 21, 40, 50 and 122°C. Additional weight loss steps are observed at 265 and 306°C of 16.1 and 24.1%. For the  $\text{Mg}_2\text{Zn}_4\text{Al}_2(\text{OH})_{16}(\text{CO}_3)\cdot 4\text{H}_2\text{O}$  hydrotalcite, the higher temperature weight loss steps are observed at 223 and 298 with weight losses of 16.6 and 14.1%. For the  $\text{Zn}_6\text{Al}_2(\text{OH})_{16}(\text{CO}_3)\cdot 4\text{H}_2\text{O}$  hydrotalcite, the higher temperature weight loss steps are observed at 208 and 428°C with weight losses of 42.8 and 9.9%. These values are close to the predicted values. These results seem to suggest that the behaviour of the Zn hydrotalcite is different from the Mg and Zn substituted Mg hydrotalcites. Mass spectrometry shows the  $\text{CO}_2$  is coming off at a much higher temperature for the Zn hydrotalcite.

### ***Mass spectrometric analyses***

The results of the mass spectra analyses of the 4 hydrotalcites of evolved water vapour and carbon dioxide are shown in Figure 3. The results of the mass loss as determined by mass spectrometry are reported in Table 2. This table also compares the weight losses as measured by mass spectrometry and by differential thermogravimetric analysis. It is a fundamental principle that the mass spectrometric curves follow the DTGA curves. This is the exacted in by comparing figures 2 with 3. The patterns are identical. The DTG curves are expressed as %/°C and the MS curves as %/time.

The mass spectrum of evolved water vapour shows that mass loss occurs for the hydrotalcite  $(\text{Mg}_6\text{Al}_2(\text{OH})_{16}(\text{CO}_3)\cdot 4\text{H}_2\text{O})$  at principally 43 and 117°C with weight losses of 2.9 and 13.0%. Whilst the temperatures of the mass loss are in excellent agreement, the weight loss for the second temperatures agrees well and this value is close to the theoretical weight loss amount of 12.0%. Two water mass determinations are measured at 246 and 258°C with a total mass loss of 49.1%. This value corresponds well with the calculated mass loss of water vapour of 45%. In the DTGA pattern a weight loss step of 18.3% is observed at 336°C. This value corresponds to the mass loss observed for the evolved  $\text{CO}_2$  gas as illustrated in Figure 3a. Two steps are observed for evolved  $\text{CO}_2$  at 258 and 339°C. This determination suggests that both water and  $\text{CO}_2$  units are lost simultaneously at 258°C.

For the  $\text{Mg}_4\text{Zn}_2\text{Al}_2(\text{OH})_{16}(\text{CO}_3)\cdot 4\text{H}_2\text{O}$  hydrotalcite, again the mass spectrum of evolved water vapour closely follows the DTGA pattern. Mass loss of evolved water vapour is observed at 52, 116 and 151°C. These temperatures are in excellent agreement with the values observed from DTGA measurements. Two water vapour determinations were made at 258 and 306°C with masses of 22.3 and 12.8%. The mass of evolved  $\text{CO}_2$  of 15.5% was observed at 329°C. Although difficult to determine from the MS patterns, it is observed that the evolved  $\text{CO}_2$  only comes off in a single step. For the  $\text{Mg}_2\text{Zn}_4\text{Al}_2(\text{OH})_{16}(\text{CO}_3)\cdot 4\text{H}_2\text{O}$  hydrotalcite, evolved water vapour is observed at 46, 130 and 145°C. The OH units are lost at 228°C, a result, which corresponds well with the value from the DTGA measurements of 223°C.  $\text{CO}_2$  is evolved at 228 and 298°C. It is apparent that the  $\text{CO}_2$  and water vapour are evolved simultaneously at 228°C. In comparison, the  $\text{Zn}_6\text{Al}_2(\text{OH})_{16}(\text{CO}_3)\cdot 4\text{H}_2\text{O}$  hydrotalcite shows carbonate decomposition at two distinct temperatures namely 198°C and at 432°C. The first temperature corresponds to the evolved water vapour at the same temperature. This again proves that both OH units and carbonate are lost simultaneously from the hydrotalcites.

## Conclusions

A series of  $\text{Mg}_6\text{Al}_2(\text{OH})_{16}(\text{CO}_3)\cdot 4\text{H}_2\text{O}$  hydrotalcites with zinc substitution have been studied by a combination of differential scanning calorimetry and high resolution thermogravimetry in combination with an evolved gas mass spectrometer. DSC shows that increased substitution of the Mg by Zn results in the shift of the heat flow steps to lower temperature. The endotherms are complex with overlapping peaks suggesting that some cation ordering occurs in the hydrotalcite structure. More steps are observed in the DSC patterns than for the DTGA. This suggests that some of the endothermic steps are surface phase related involving changes in the hydroxyl surface structure.

High resolution DTGA combined with mass spectrometry shows that the temperature of the dehydroxylation of the hydrotalcite decreases with increased Zn composition. Three principal weight loss steps are observed (a) loss of adsorbed water in the 40 to 50°C temperature range (b) loss of water between 110 and 150°C (c) dehydroxylation in the 200 to 248°C (d) loss of carbonate in the 300 to 350°C temperature range. The results of these thermal analyses show that hydrotalcites are well suited for the inclusion in nano-composites. The hydrotalcites are stable to quite high temperatures compared with the temperature of polymerisation. Thermally treated hydrotalcites provide metal oxides for incorporation into the nanocomposite.

## Acknowledgments

The Centre for Instrumental and Developmental Chemistry, of the Queensland University of Technology is gratefully acknowledged for financial, and infra-structural support for this project. The ARC (Australian Research Council) is thanked for the funding for the thermal analysis facility.

## References

- 1 J. Theo Kloprogge and R. L. Frost, Appl. Catal., A, 184, (1999) 61.
- 2 J. Theo Kloprogge and R. L. Frost, Phys. Chem. Chem. Phys., 1, (1999) 1641.

- 3 S. W. Rhee, M.-J. Kang, and H. Moon, *J. Korean Chem. Soc.*, 39, (1995) 627.
- 4 G. J. Ross and H. Kodama, *Am. Mineral.*, 52, (1967) 1036.
- 5 C. W. Beck, *Am. Mineralogist*, 35, (1950) 985.
- 6 G. W. Brindley and S. Kikkawa, *Clays Clay Miner.*, 28, (1980) 87.
- 7 S. Caillere, *Compt. rend.*, 219, (1944) 256.
- 8 P. Bera, M. Rajamathi, M. S. Hegde, and P. V. Kamath, *Bull. Mater. Sci.*, 23, (2000) 141.
- 9 G. Camino, A. Maffezzoli, M. Braglia, M. De Lazzaro, and M. Zammarano, *Polym. Degrad. Stab.*, 74, (2001) 457.
- 10 K. Chigiri and Y. Azuma, *Jpn. Kokai Tokkyo Koho*, (Hien Denko K. K., Japan), Jp, 2000.
- 11 L. Hickey, J. T. Klopogge, and R. L. Frost, *J. Mater. Sci.*, 35, (2000) 4347.

**Table 1 Results of the heat flow results from the DSC for hydrotalcites**

<b>Hydrotalcites Temp°C/ %heat Flow</b>	<b>Mg/Zn 1:0</b>	<b>Mg/Zn 4:2</b>	<b>Mg/Zn 2:4</b>	<b>Mg/Zn 0:1</b>
Heat Flow Step 1	38 0.5	47 0.3		41 0.5
Heat Flow Step 2	57 9.6	75 25.2	69 3.4	58 1.9
Heat Flow Step 3			91 16.8	67 2.5
Heat Flow Step 4	87 3.2	93 17.9	98 5.5	
Heat Flow Step 5	98 2.5		105 6.7	108 4.9
Heat Flow Step 6	131 11.0	124 0.5		
Heat Flow Step 7		144 5.5		161 18.4
Heat Flow Step 8		172 5.6	174 15.3	178 11.2
Heat Flow Step 9		184 7.0	186 8.3	186 1.8
Heat Flow Step 10			196 2.8	218 8.5
Heat Flow Step 11	256 21.5	260 15.0	250 8.5	238 14.1
Heat Flow Step 12	260 9.7			
Heat Flow Step 13	269 8.6			
Heat Flow Step 14	340 14.2	317 13.4	321 26.6	309 20.4
Heat Flow Step 15	352 2.0	329 3.8		

**Table 2 Results of the weight losses of the DTG and MS for hydrotalcites**

Hydrotalcites	Mg/Zn 1:0		Mg/Zn 4:2		Mg/Zn 2:4		Mg/Zn 0:1	
	DTG	MS	DTG	MS	DTG	MS	DTG	MS
Temperature/°C	36	37	21	37	25	34	25	30
Weight Loss/gain Step 1	3.9	1.7	4.5	4.8	16.1	4.9	3.6	2.5
Temperature/°C	40	43	40	44	39	39	31	33
Weight Loss Step 2	21.0	2.9	7.2	5.3	20.0	4.9	0.2	3.6
Temperature/°C	84	84	50	52	49	46	63	72
Weight Loss Step 3	7.3	1.3	7.6	19.9	7.6	15.3	0.8	0.7
Temperature/°C	112	117	122	116	98	107	131	135
Weight Loss Step 4	12.3	13.0	9.1	4.4	4.1	2.2	25.6	41.1
Temperature/°C			148	151	127	130	147	148
Weight Loss Step 5			3.0	7.7	7.3	11.3	7.7	9.9
Temperature/°C					144	145	155	155
Weight Loss Step 6					5.3	14.4	3.9	4.6
Temperature/°C					174	174	196	198
Weight Loss Step 7					3.5	0.2	5.5	30.9
Temperature/°C							208	209
Weight Loss Step 8							42.8	1.1
Temperature/°C	246	246			223	228		
Weight Loss Step 9	19.6	31.0			16.6	34.4		
Temperature/°C	261	258	265	258				
Weight Loss Step 10	14.6	18.1	16.1	22.3				
Temperature/°C	307	304	306	306	298	298		
Weight Loss Step 11	3.0	1.4	24.1	12.8	14.1	4.6		
Temperature/°C	336	339	347	329				432
Weight Loss Step 12	18.3	8.1	11.3	15.5				24.2

## **List of Tables**

**Table 1 Results of the heat flow results from the DSC for hydrotalcites**

**Table 2 Results of the weight losses of the DTG and MS for hydrotalcites**

## **List of Figures**

**Figure 1 Differential Scanning Calorimetry of Mg/Zn hydrotalcites**

**Figure 2 High Resolution DGTA of Mg/Zn hydrotalcites**

**Figure 3a (a) MS of evolved water vapour (b) MS of evolved CO<sub>2</sub> (c) DTGA curve for Mg/Al hydrotalcite**

**Figure 3b (a) MS of evolved water vapour (b) MS of evolved CO<sub>2</sub> (c) DTGA curve for 4:2 Mg-Zn/Al hydrotalcite**

**Figure 3c (a) MS of evolved water vapour (b) MS of evolved CO<sub>2</sub> (c) DTGA curve for 2:4 Mg-Zn/Al hydrotalcite**

**Figure 3d (a) MS of evolved water vapour (b) MS of evolved CO<sub>2</sub> (c) DTGA curve for Zn/Al hydrotalcite**

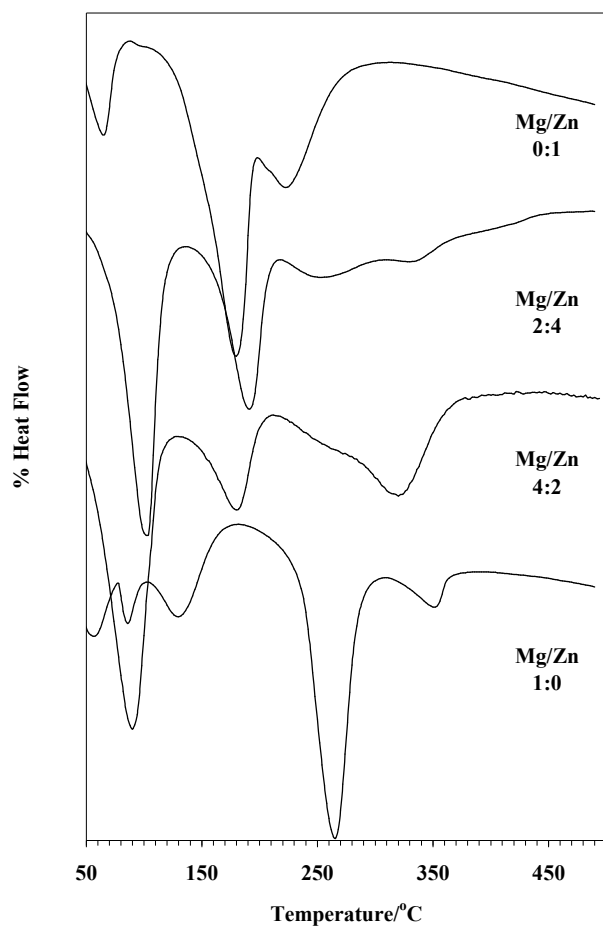


**Figure 1**

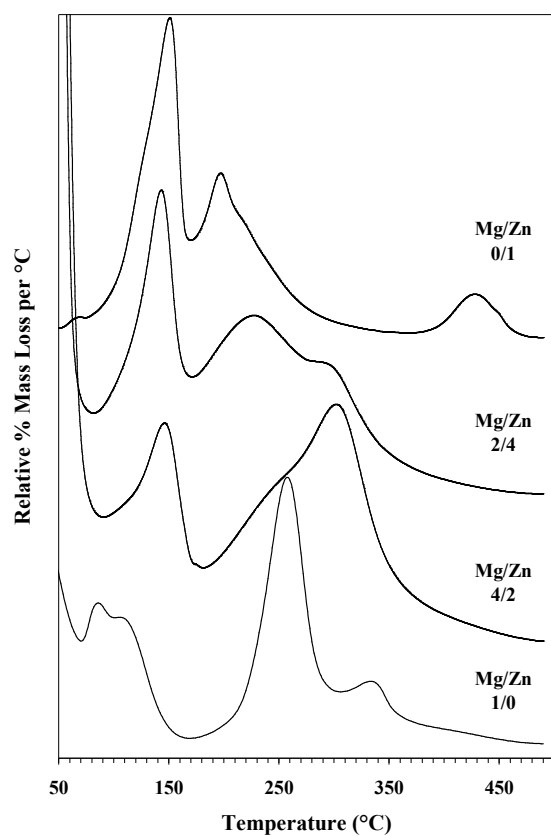


**Figure 2**

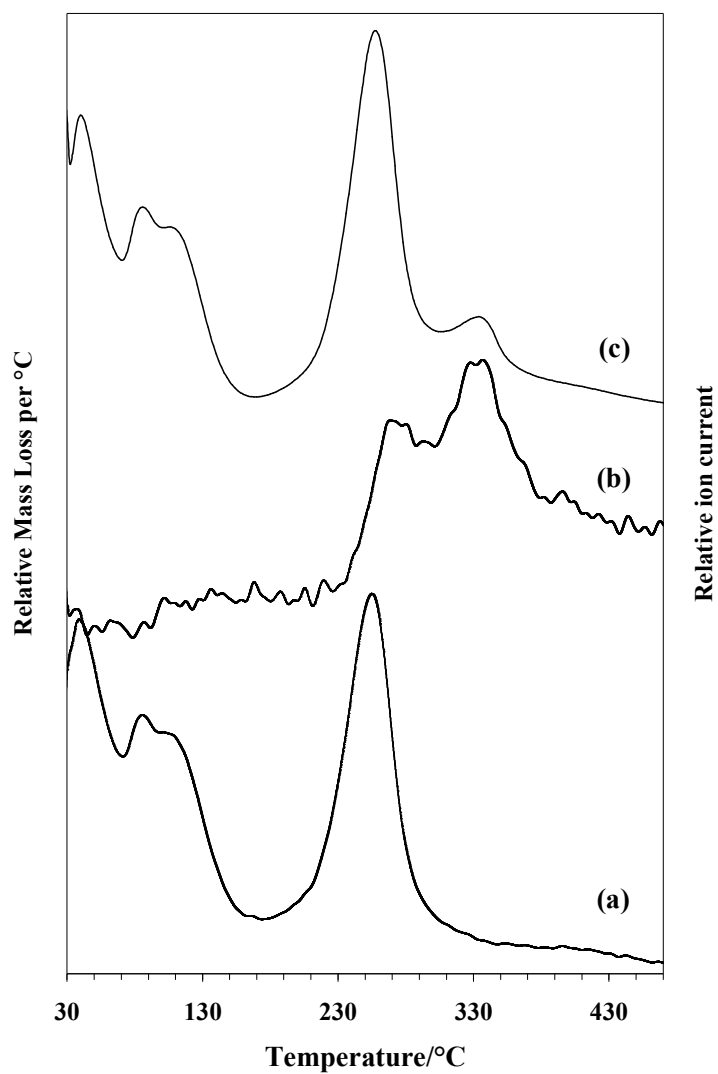
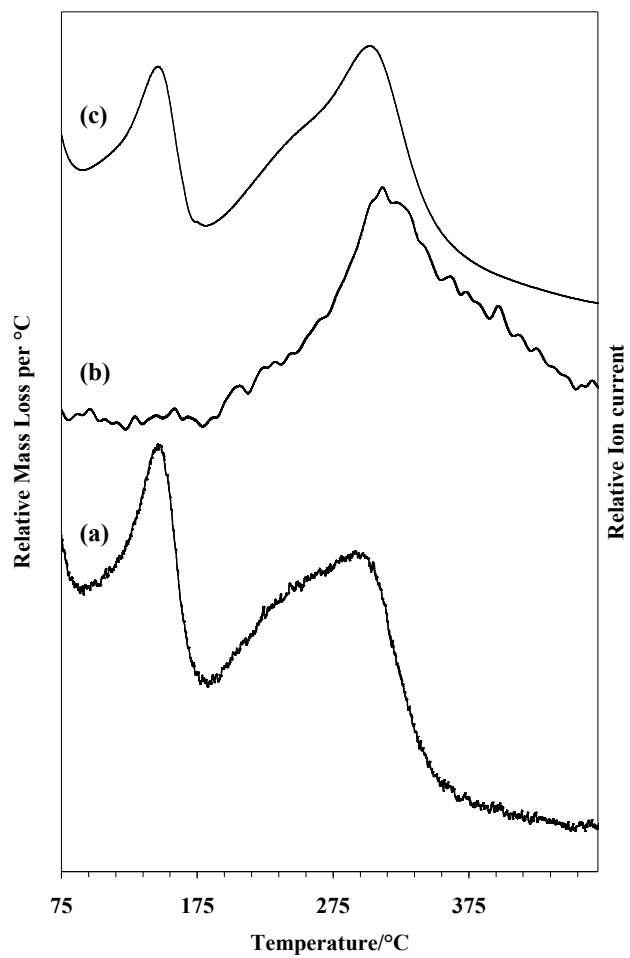


Figure 3a



**Figure 3b**

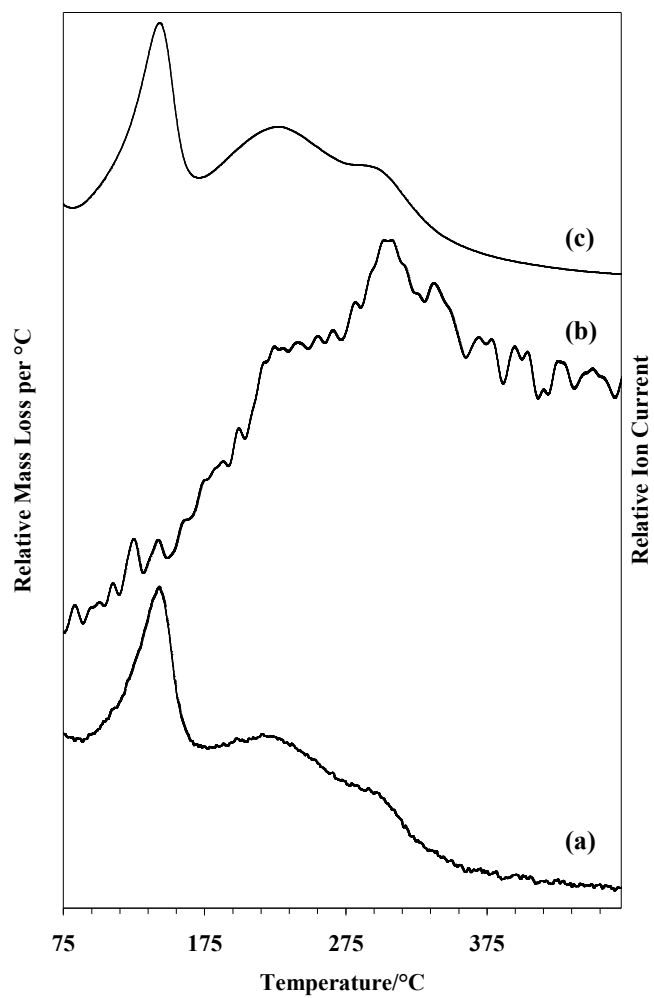
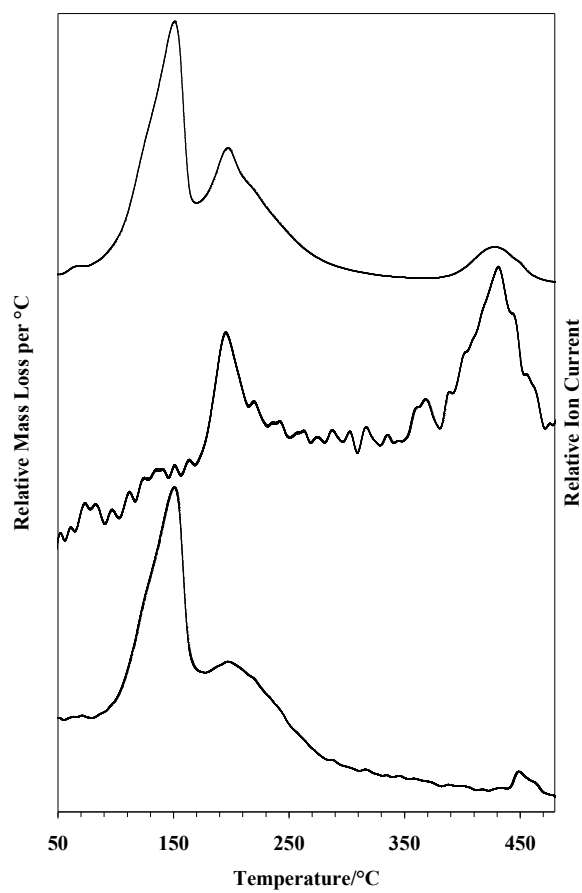


Figure 3c



**Figure 3d**

